26. Neutrinos in Cosmology

Revised August 2025 by J. Lesgourgues (TTK, RWTH) and L. Verde (ICC, U. of Barcelona; ICREA, Barcelona).

26.1 Standard neutrino cosmology

Neutrinos leave detectable imprints on cosmological observations that can then be used to constrain neutrino properties. This is a great example of the remarkable interconnection and interplay between nuclear physics, particle physics, astrophysics, and cosmology (for general reviews see e.g., [1–4]). Present cosmological data are already providing constraints on neutrino properties that are not only complementary but also competitive with terrestrial experiments; for instance, upper bounds on the total neutrino mass have shrunk by about an order of magnitude in the past two decades. Forthcoming cosmological data may soon provide key information, not obtainable in other ways like e.g., a measurement of the absolute neutrino mass scale.

A relic neutrino background pervading the Universe (the Cosmic Neutrino background, $C\nu B$) is a generic prediction of the standard hot Big Bang model (see Big Bang Nucleosynthesis – Chap. 24 of this Review). While it has not yet been detected directly, it has been indirectly confirmed by the accurate agreement of predictions and observations of: a) the primordial abundance of light elements (see Big Bang Nucleosynthesis – Chap. 24) of this Review; b) the power spectrum of Cosmic Microwave Background (CMB) anisotropies (see Cosmic Microwave Background – Chap. 29 of this Review); and c) the large-scale clustering of cosmological structures. Within the hot Big Bang model such good agreement would fail dramatically without a $C\nu B$ with properties matching closely those predicted by the standard neutrino decoupling process (i.e., involving only weak interactions).

We will illustrate below that cosmology is sensitive to the following neutrino properties: their density, related to the number of active (i.e., left-handed, see Neutrino Mass, Mixing, and Oscillations – Chap. 14 of this Review) neutrino species, and their masses. At first order, cosmology is sensitive to the total neutrino mass, but is blind to the mixing angles and CP violation phase as discussed in Neutrino Mass, Mixing, and Oscillations (Chap. 14 of this Review). This makes cosmological constraints nicely complementary to measurements from terrestrial neutrino experiments.

The minimal cosmological model, Λ CDM, currently providing a good fit to most cosmological data sets (with the exception of some data in tension, discussed in The Cosmological Parameters Chap. 25 of this Review), assumes that the only massless or light (sub-keV) relic particles since the Big Bang Nucleosynthesis (BBN) epoch are photons and active neutrinos. Extended models with light sterile neutrinos, light thermal axions or other light relics—sometimes referred to as "dark radiation"— would produce effects similar to, and potentially degenerate with, those of active neutrinos. Thus neutrino bounds are often discussed together with limits on such scenarios. In the case of observational evidence for an unexpected density of radiation, it might not be obvious to discriminate between interpretation in terms of active neutrinos with non-standard decoupling, additional production mechanisms, non-standard interactions, etc., or in terms of some additional light particles. Such extensions have been explored as a possible way to resolve the H_0 tension between late and early Universe determinations [5–8], but are not widely favoured [9–13].

Neutrino density and mass bounds can be derived under the assumption of no additional massless or light relic particles, and the neutrino density measured in that way provides a test of standard (*i.e.*, involving only weak interactions) neutrino decoupling.

In that model, the three active neutrino types thermalize in the early Universe, with a negligible leptonic asymmetry. Then they can be viewed as three propagating mass eigenstates sharing the same temperature and identical Fermi-Dirac distributions, thus with no visible effects of flavour

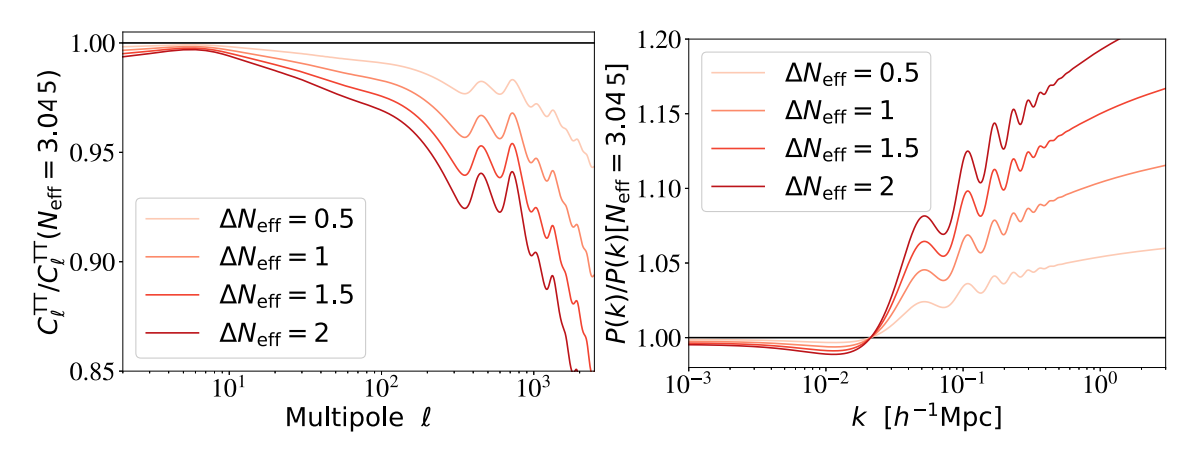


Figure 26.1: Ratio of the CMB C_{ℓ}^{TT} (left, including lensing effects) and matter power spectrum P(k) (right, computed for each model in units of $(h^{-1}\mathrm{Mpc})^3$) for different values of $\Delta N_{\mathrm{eff}} \equiv N_{\mathrm{eff}} - 3.044$ over those of a reference model with $\Delta N_{\mathrm{eff}} = 0$. In order to minimize and better characterize the effect of N_{eff} on the CMB, the parameters that are kept fixed are $\{z_{\mathrm{eq}}, z_{\Lambda}, \omega_{\mathrm{b}}, \tau\}$ and the primordial spectrum parameters. Fixing $\{z_{\mathrm{eq}}, z_{\Lambda}\}$ is equivalent to fixing the fractional density of total radiation, of total matter, and of cosmological constant $\{\Omega_{\mathrm{r}}, \Omega_{\mathrm{m}}, \Omega_{\Lambda}\}$, while increasing the Hubble parameter as a function of N_{eff} . The statistical errors on the C_{ℓ} are about 1% for a band power of $\Delta \ell = 30$ at $\ell \sim 1000$. The error on P(k) is estimated to be of the order of 5%.

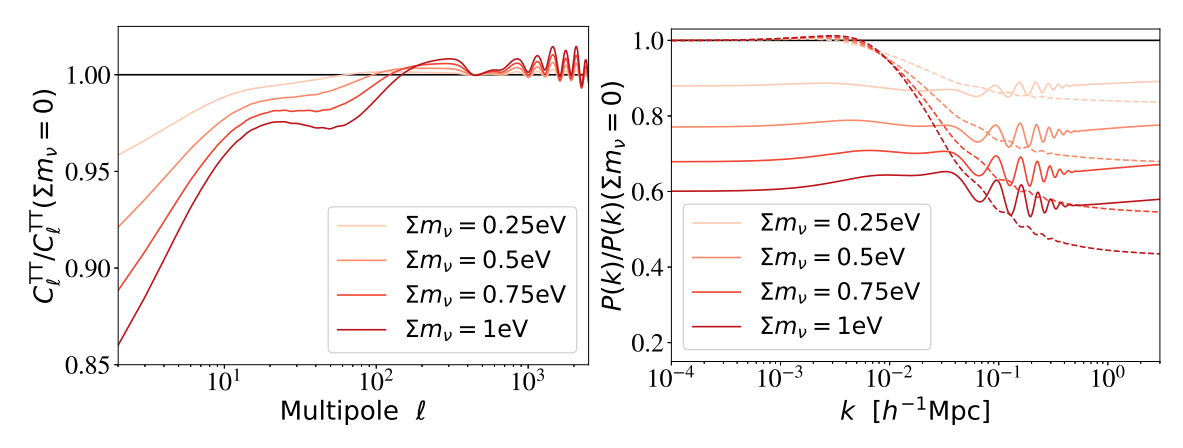


Figure 26.2: Ratio of the CMB C_{ℓ}^{TT} and matter power spectrum P(k) (computed for each model in units of $(h^{-1}\mathrm{Mpc})^3$) for different values of $\sum m_{\nu}$ over those of a reference model with massless neutrinos. In order to minimize and better characterise the effect of $\sum m_{\nu}$ on the CMB, the parameters that are kept fixed are $\omega_{\rm b}$, $\omega_{\rm c}$, τ , the angular scale of the sound horizon $\theta_{\rm s}$ and the primordial spectrum parameters (solid lines). This implies that we are increasing the Hubble parameter h as a function of $\sum m_{\nu}$. For the matter power spectrum, in order to single out the effect of neutrino free-streaming on P(k), the dashed lines show the spectrum ratio when $\{\omega_{\rm m}, \omega_{\rm b}, \Omega_{\Lambda}\}$ are kept fixed. For comparison, the error on P(k) is of the order of 5% with current observations, and the fractional C_{ℓ} errors are of the order of $1/\sqrt{\ell}$ at low ℓ .

oscillations. Neutrinos decouple gradually from the thermal plasma at temperatures $T \sim 2$ MeV. In the instantaneous neutrino decoupling limit, *i.e.*, assuming that neutrinos were fully decoupled at the time when electron-positrons annihilate and release entropy in the thermal bath, the neutrino-to-photon density ratio between the time of electron-positron annihilation and the non-relativistic

transition of neutrinos would be given by

$$\frac{\rho_{\nu}}{\rho_{\gamma}} = \frac{7}{8} N_{\text{eff}} \left(\frac{4}{11}\right)^{4/3} , \qquad (26.1)$$

with $N_{\rm eff}=3$, and the last factor comes from the fourth power of the temperature ratio $T_{\nu}/T_{\gamma}=$ $(4/11)^{1/3}$ (see Big Bang Cosmology – Chap. 22 in this *Review*). In the above formula, N_{eff} is called the effective number of neutrino species because it can be viewed as a convenient parameterization of the relativistic energy density of the Universe beyond that of photons, in units of one neutrino in the instantaneous decoupling limit. Precise simulations of neutrino decoupling and electron-positron annihilation, taking into account flavor oscillations, provide accurate predictions for the actual phase-space distribution of relic neutrinos [14–22]. These distributions differ from the instantaneous decoupling approximation through a combination of a small shift in the photon temperature and small flavor-dependent non-thermal distortions, all at the percent level. The final result for the density ratio ρ_{ν}/ρ_{γ} in the relativistic regime can always be expressed as in Eq. (26.1), but with a different value of $N_{\rm eff}$. The most recent analyses, which include the effect of neutrino oscillations with the present values of the mixing parameters, an improved calculation of the collision terms, and the most recent results on plasma thermodynamics QED corrections, give $N_{\text{eff}} = 3.044$ [18,19,21,22]. The precise number density ratio n_{ν}/n_{γ} can also be derived from such studies, and is important for computing $\Omega_{\nu}h^2/\sum_i m_i$ (ratio of the physical density of neutrinos in units of the critical density to the sum of neutrino masses) in the non-relativistic regime. Once neutrinos are decoupled, their momentum redshifts like $p \propto 1/a$ but, due to the absence of interactions, their phase-space distributions remain constant when expressed in terms of the comoving momentum q = pa, even when they become non-relativistic.

The neutrino temperature today, $T_{\nu}^{0} \simeq 1.7 \times 10^{-4} \,\mathrm{eV} \simeq 1.9 \,\mathrm{K}$, is smaller than at least two of the neutrino masses, since the two squared-mass differences are $|\Delta m_{31}^{2}|^{1/2} > |\Delta m_{21}^{2}|^{1/2} > T_{\nu}^{0}$ (see Neutrino mass, Mixing, and oscillations – Chap. 14 of this *Review*). Thus at least two neutrino mass eigenstates are non-relativistic today and behave as a small "hot" fraction of the total dark matter (they cannot be all the dark matter, as explained in Chap. 27 of this *Review*). This fraction of hot dark matter can be probed by cosmological experiments, for two related reasons, as we now describe.

First, neutrinos are the only known particles behaving as radiation at early times (during the CMB acoustic oscillation era) and dark matter at late times (during structure formation), which has consequences on the background evolution. Neutrinos become non-relativistic when their mass is equal to their average momentum, given for any Fermi-Dirac-distributed particle by $\langle p \rangle = 3.15\,T$. Thus the redshift of the non-relativistic transition is given by $z_i^{\rm nr} = m_i/(3.15\,T_\nu^0)-1=m_i/[0.53\,{\rm meV}]-1$ for each eigenstate of mass m_i , giving for instance $z_i^{\rm nr}=110$ for $m_i=60\,{\rm meV}$, corresponding to a time deep inside the matter-dominated regime. Second, until the non-relativistic transition, neutrinos travel at the speed of light, and later on they move at a typical velocity $\langle v_i/c \rangle = 3.15\,T_\nu(z)/m_i = 0.53(1+z)\,{\rm meV}/m_i$, which is several orders of magnitude larger than that of the dominant cold (or even of possibly warm) dark matter component(s). This brings their characteristic diffusion scale, called the "free-streaming length", to cosmological relevant values, with consequences for gravitational clustering and the growth of structure.

Once neutrinos are non-relativistic, their energy density is given by $\rho_{\nu} \simeq \sum m_i n_i$. Since the number densities n_i are equal to each other (up to negligible corrections coming from flavor effects in the decoupling phase), the total mass $\sum m_{\nu} = m_1 + m_2 + m_3$ can be factored out. It is possible that the lightest neutrino is still relativistic today, in which case this relation is slightly incorrect, but given that the total density is always strongly dominated by that of non-relativistic neutrinos, the

error made is completely negligible. Using the expression for n_i/n_{γ} obtained from precise neutrino decoupling studies [18, 19], and knowing n_{γ} from the measurement of the CMB temperature, one can compute ρ_{ν}^{0} , the total neutrino density today, in units of the critical density ρ_{crit}^{0} :

$$\Omega_{\nu} = \frac{\rho_{\nu}^{0}}{\rho_{\text{crit}}^{0}} = \frac{\sum m_{\nu}}{93.12h^{2} \,\text{eV}},$$
(26.2)

and the total neutrino average number density today: $n_{\nu}^0=339.5~{\rm cm}^{-3}$ [23]. Here h is the Hubble constant in units of 100 km s⁻¹ Mpc⁻¹.

26.2 Effects of neutrino properties on cosmological observables

As long as they are relativistic, i.e., until some time deep inside the matter-dominated regime for neutrinos with a mass $m_i \ll 3.15\,T_{\nu}^{\rm eq} \simeq 1.5\,{\rm eV}$ (see Big Bang Cosmology, Chap. 22 in this Review), neutrinos enhance the density of radiation: this effect is parameterized by $N_{\rm eff}$ and can be discussed separately from the effect of the mass that will be described later in this section. Increasing $N_{\rm eff}$ impacts the observable spectra of CMB anisotropies and matter fluctuations through background and perturbation effects.

26.2.1 Effect of $N_{\rm eff}$ on the CMB

The background effects depend on what is kept fixed when increasing N_{eff} . If the densities of other species are kept fixed, a higher N_{eff} implies a smaller redshift of radiation-to-matter equality, with very strong effects on the CMB spectrum: when the amount of expansion between radiationto-matter equality and photon decoupling is larger, the CMB acoustic peaks are suppressed. This effect is not truly characteristic of the neutrino density, since it can be produced by varying several other parameters. Hence, to characterize the effect of $N_{\rm eff}$, it is more useful and illuminating to enhance the density of total radiation, of total matter, and of Λ by exactly the same amount, in order to keep the redshift of radiation-to-matter equality $z_{\rm eq}$ and matter-to- Λ equality z_{Λ} fixed [24–27]. The primordial spectrum parameters, the baryon density $\omega_{\rm b} \equiv \Omega_{\rm b} h^2$ and the optical depth to reionization τ can be kept fixed at the same time, since we can simply vary $N_{\rm eff}$ together with the Hubble parameter h with fixed $\{\omega_{\rm b}, \Omega_{\rm c}, \Omega_{\Lambda}\}$. The impact of such a transformation is shown in Fig. 26.1 for the CMB temperature spectrum C_{ℓ}^{TT} (defined in Chap. 29 in this *Review*) and for the matter power spectrum P(k) (defined in Chap. 22 in this Review) for several representative values of $N_{\rm eff}$. These effects are within the reach of cosmological observations given current uncertainties, as discussed in Section 26.3.1 (for instance, with the *Planck* satellite data, the statistical error on the C_{ℓ} s is of the order of one per cent for a band power of $\Delta \ell = 30$ at $\ell \sim 1000$).

With this transformation, the main background effect of $N_{\rm eff}$ is an increase in the diffusion scale (or Silk damping scale, see Cosmic Microwave Background – Chap. 29 in this Review) at the time of decoupling, responsible for the decrease in C_ℓ^{TT} at high ℓ , plus smaller effects coming from a slight increase in the redshift of photon decoupling [24–27]. At the level of perturbations, a higher $N_{\rm eff}$ implies that photons feel gravitational forces from a denser neutrino component; this tends to decrease the acoustic peaks (because neutrinos are distributed in a smoother way than photons) and to shift them to larger scales, *i.e.*, smaller multipoles (because photon perturbations traveling at the speed of sound in the photon-baryon fluid feel some dragging effect from neutrino perturbations travelling at the speed of light) [24,26–28]. The effect of increasing $N_{\rm eff}$ on the polarization spectrum features are the same as on the temperature spectrum: an increased Silk damping, and a shift in the acoustic peak amplitude and location – the latter effect is even more clear in the polarization spectrum, in which the location of acoustic peaks does not get further influenced by a Doppler

¹The value 93.12 eV applies to the limit of large masses, in which $\rho_{\nu}^{0} = \sum m_{i} n_{i}^{0}$ and neutrinos are degenerate in mass [23]. This number would be larger by about 0.1% in the limit of minimal normal hierarchy (or smaller by about 0.06% for minimal inverted hierarchy), due the lightest mass state(s) being still relativistic today and to flavor-dependent non-thermal distortions in the neutrino phase-space distributions.

effect like for temperature. The combination of these effects is truly characteristic of the radiation density parameter $N_{\rm eff}$ and cannot be mimicked by other parameters; thus $N_{\rm eff}$ can be accurately measured from the CMB alone. However, there are correlations between $N_{\rm eff}$ and other parameters. In particular, we have seen (Fig. 26.1) that in order to minimize the effect of $N_{\rm eff}$ on the CMB spectrum, one should vary h at the same time, hence there is a correlation between $N_{\rm eff}$ and h, which implies that independent measurements reducing the error bar on h also reduce that on $N_{\rm eff}$. Note that this correlation is not a perfect degeneracy, so both parameters can be constrained with CMB data alone.

26.2.2 Effect of $N_{\rm eff}$ on the matter spectrum

We have discussed the effect of increasing $N_{\rm eff}$ while keeping $z_{\rm eq}$ and $\omega_{\rm b}$ fixed, because the latter two quantities are very accurately constrained by CMB data. This implies that $\omega_{\rm c}$ increases with $N_{\rm eff}$, and that the ratio $\omega_{\rm b}/\omega_{\rm c}=\Omega_{\rm b}/\Omega_{\rm c}$ decreases. However, the ratio of baryonic-to-dark matter has a strong impact on the shape of the matter power spectrum, because until the time of decoupling of the baryons from the photons, CDM experiences gravitational collapse, while baryons are kept smoothly distributed by photon pressure and affected by acoustic oscillations. The decrease of $\Omega_{\rm b}/\Omega_{\rm c}$ following from the increase of $N_{\rm eff}$ gives more weight to the most clustered of the two components, namely the dark matter, and produces an enhancement of the small-scale matter power spectrum and a damping of the amplitude of baryon acoustic oscillations (BAOs), clearly visible in Fig. 26.1 (right plot). The scale of BAOs is also slightly shifted by the same neutrino dragging effect as for CMB peaks [24,29].

The increase in the small-scale matter power spectrum is also responsible for a last effect on the CMB power spectra: the CMB last-scattering surface is slightly more affected by weak lensing from large-scale structures. This tends to smooth the maxima, the minima, and the damping scale of the CMB spectra [30].

26.2.3 Effect of neutrino masses on the CMB

Neutrino eigenstates with a mass $m_i \ll 0.6 \, \mathrm{eV}$ become non-relativistic after photon decoupling. They contribute to the non-relativistic matter budget today, but not at the time of equality or recombination. If we increase the neutrino mass while keeping fixed the density of baryons and dark matter (ω_b and ω_c), the early cosmological evolution remains fixed and independent of the neutrino mass, until the time of the non-relativistic transition. Thus one might expect that the CMB temperature and polarization power spectra are left invariant. This is not true for four reasons [26, 31, 32]

First, the neutrino density enhances the total non-relativistic density at late times, $\omega_{\rm m} = \omega_{\rm b} + \omega_{\rm c} + \omega_{\nu}$, where $\omega_{\nu} \equiv \Omega_{\nu} h^2$ is given as a function of the total mass $\sum m_{\nu}$ by Eq. (26.2). The late background evolution impacts the CMB spectrum through the relation between scales on the last-scattering surface and angles on the sky, and through the late ISW effect (see Cosmic Microwave Background – Chap. 29 of this Review). These two effects depend, respectively, on the angular diameter distance to recombination, $d_{\rm A}(z_{\rm rec})$, and on the redshift of matter-to- Λ equality. Increasing $\sum m_{\nu}$ tends to modify these two quantities. By playing with h and Ω_{Λ} , it is possible to keep one of them fixed, but not both at the same time. Since the CMB measures the angular scale of acoustic oscillations with exquisite precision, and is only loosely sensitive to the late ISW effect due to cosmic variance, we choose in Fig. 26.2 to vary the Hubble parameter in order to maintain a fixed scale $d_{\rm A}(z_{\rm rec})$. With such a choice, an increase in neutrino mass comes together with a decrease in the late ISW effect explaining the depletion of the CMB spectrum for $\ell \leq 20$. The fact that both $\sum m_{\nu}$ and h enter the expression of $d_{\rm A}(z_{\rm rec})$ implies that measurements of the neutrino mass from CMB data are strongly correlated with h. Second, the non-relativistic transition of neutrinos affects the total pressure-to-density ratio of the Universe, and causes a small variation

of the metric fluctuations. If this transition takes place not too long after photon decoupling, the variation is observable through the early ISW effect [26, 31, 33]. It is responsible for the dip seen in Fig. 26.2 for $20 \le \ell \le 200$. Third, when the neutrino mass is higher, the CMB spectrum is less affected by the weak lensing effect induced by the large-scale structure at small redshifts. This is due to a decrease in the matter power spectrum described in the next paragraphs. This reduced lensing effect is responsible for most of the oscillatory patterns visible in Fig. 26.2 (left plot) for $\ell \ge 200$. Fourth, the neutrinos with the smallest momenta start to become non-relativistic earlier than the average ones. The photon perturbations feel this through their gravitational coupling with neutrinos. This leads to a small enhancement of C_l^{TT} for $\ell \ge 500$, which is hardly visible on Fig. 26.2 because it is balanced by the lensing effect.

26.2.4 Effect of neutrino masses on the matter spectrum

The physical effect of neutrinos on the matter power spectrum is related to their velocity dispersion. Neutrinos free-stream over large distances without falling into small potential wells. The free-streaming scale is roughly defined as the distance traveled by neutrinos over a Hubble time scale $t_{\rm H}=(a/\dot{a})$, and approximates the scale below which neutrinos remain very smooth. On larger scales, they cluster in the same way as cold dark matter. The power spectrum of total matter fluctuations, related to the squared fluctuation $\delta_{\rm m}^2$ with $\delta_{\rm m}\equiv\delta_{\rm b}+\delta_{\rm c}+\delta_{\nu}$, gets a negligible contribution from the neutrino component on small scales, and is reduced by a factor $(1-2f_{\nu})$, where $f_{\nu}=\omega_{\nu}/\omega_{\rm m}$. Additionally, on scales below the free-streaming scale, the growth of ordinary cold dark matter and baryon fluctuations is modified by the fact that neutrinos contribute to the background density, but not to the density fluctuations. This changes the balance between the gravitational forces responsible for clustering, and the Hubble friction term slowing it down. Thus the growth rate of CDM and baryon fluctuations is reduced [34]. This results today in an additional suppression of the small-scale linear matter power spectrum by approximately $(1-6f_{\nu})$. These two effects sum up to a factor $(1-8f_{\nu})$ [35] (more precise approximations can be found in Refs. [2,26]). The non-linear spectrum is even more suppressed on mildly non-linear scales [3, 36–40].

This effect is often illustrated by plots of the matter power spectrum ratio with fixed parameters $\{\omega_{\rm m}, \omega_{\rm b}, \Omega_{\Lambda}\}$ and varying f_{ν} , i.e., with the CDM density adjusted to get a fixed total dark matter density [2, 26, 35] (see Fig. 26.2, right plot, dashed lines). This transformation does not leave the redshift of equality $z_{\rm eq}$ invariant, and has very large effects on the CMB spectra. If one follows the logic of minimizing CMB variations and fixing $z_{\rm eq}$ like in the previous paragraphs, the increase in $\sum m_{\nu}$ must take place together with an increase of h, which tends to suppress the large-scale power spectrum, by approximately the same amount as the neutrino free-streaming effect [41]. In that case, the impact of neutrino masses on the matter power spectrum appears as an overall amplitude suppression, which can be seen in Fig. 26.2 (right plot, solid lines). The oscillations on intermediate wavenumbers come from a small shift in the BAO scale [41]. This global effect is not degenerate with a variation of the primordial spectrum amplitude $A_{\rm s}$, because it only affects the matter power spectrum, and not the CMB spectra. However, the amplitude of the CMB temperature and polarization spectrum is given by the combination $A_{\rm s}e^{-2\tau}$. Hence a measurement of τ is necessary in order to fix $A_{\rm s}$ from CMB data, and avoid a parameter degeneracy between $\sum m_{\nu}$ and $A_{\rm s}$ [41–43].

A few of the neutrino mass effects described above – free-streaming scale, early ISW – depend on individual masses m_i , but most of them depend only on the total mass through f_{ν} – suppression of the matter power spectrum, CMB lensing, and shift in angular diameter distance. Because the latter effects are easier to measure, cosmology is primarily sensitive to the total mass $\sum m_{\nu}$ [44, 45]. The possibility that future data sets might be able to measure individual masses or the mass hierarchy, despite systematic errors and parameter degeneracies, is still an active subject of investigation [46–52].

26.3 Cosmological constraints on neutrino properties

In this chapter we focus on cosmological constraints on the abundance and mass of ordinary active neutrinos. Several stringent but model dependent constraints on non-standard neutrinos (e.g., sterile neutrinos, active neutrinos with interactions beyond the weak force, unstable neutrinos with invisible decay, etc.) can also be found in the literature.

We highlight that cosmological constraints on neutrino properties are always obtained within the framework of a Λ CDM model or simple and popular extensions of this model, as spelled out in the following subsections. In light of the emergence of cosmological tensions – especially the so-called Hubble tension (see Chap. 25 of this Review), as well as hints of a possible tension on the late expansion history (see Chap. 28 of this Review) – it is important to bear in mind the following considerations. Inconsistent measurements should not be combined: bounds obtained from combination of discrepant data sets should be considered with extreme caution. Additionally, the constraints reported below assume that the solution of the H_0 tension – whatever that may be – leaves the interpretation of the adopted probes unaffected.

Model N_{eff} Ref. CMB alone $\overline{\Lambda {
m CDM}} + N_{
m eff}$ Pl18[T&E] 2.92 ± 0.18 (68%CL) [53]Pl18[T&E]+ACT[T&E] $\Lambda \text{CDM} + N_{\text{eff}}$ $2.73 \pm 0.14 \ (68\%CL)$ [54]P118[T&E] + ACT[T&E] + SPT-3G[T&E, lensing] $\Lambda \text{CDM} + N_{\text{eff}}$ $2.81 \pm 0.12 \ (68\%CL)$ [55] $\overline{\text{CMB}} + \text{BAO}$ SPT-3G[T&E,lensing]+DESI-DR2 $\Lambda \text{CDM} + N_{\text{eff}}$ $3.52 \pm 0.23 \ (68\% \ CL)$ [55] $\Lambda \text{CDM} + N_{\text{eff}}$ Pl18[T&E]+ACT[T&E,lensing]+DESI-DR1 $2.86 \pm 0.13 \ (68\% \ CL)$ [54]Pl18[T&E]+ACT[lensing]+DESI-DR2 $w_0 w_a \text{CDM} + N_{\text{eff}}$ $2.96 \pm 0.18 \ (68\% \ CL)$ [56]

Table 26.1: Summary of N_{eff} constraints.

26.3.1 Neutrino abundance

Table 26.1 shows a list of constraints on $N_{\rm eff}$ obtained with several combinations of data sets. 'Pl18' denotes the *Planck* 2018 data [53], 'ACT' the Data Release 6 (DR6) of the Atacama Cosmology Telescope [54], and 'SPT-3G' the Data 1 (D1) release of the South Pole Telescope [55]. These data sets are composed of temperature and polarization likelihoods (T&E) and CMB lensing likelihoods (lensing) based on lensing extraction from quadratic estimators.² 'DESI-DR1' and 'DESI-DR2' refer to measurements of the BAO scale (and hence of the angular diameter distance) from the Data Release 1 or 2 of the Dark Energy Spectroscopic Instrument (DESI) [57].

Within the framework of a 7-parameter cosmological model (Λ CDM+ $N_{\rm eff}$), the constraint on $N_{\rm eff}$ from the Planck 2018 data release [TT,TE,EE+lowE] is $N_{\rm eff} = 2.92^{+0.36}_{-0.37}$ (95%CL). This number is perfectly compatible with the prediction of the standard neutrino decoupling model, $N_{\rm eff} = 3.044$, and also with bounds on $N_{\rm eff}$ from Big Bang Nucleosynthesis and primordial element abundances (see Chapter 24 of this Review). This can be viewed as a proof of self-consistency of the cosmological model.

The bounds can be tightened by adding information from ground-based CMB experiments probing higher ℓ , CMB lensing (second and third line in the table), and complementary information on the low-redshift background expansion from BAOs (lower section of the table). While the

 $^{^2}$ The CMB lensing likelihoods used in Refs. [54–56] are based on different combinations of *Planck*, ACT, and SPT-3G data.

exact central values and error-bars might depend slightly on the choice of CMB likelihood, all combinations of *Planck* 2018 data with additional CMB and/or BAO data reported in Table 26.1 return measurements consistent with the standard expectation at the 95% confidence level. The only marginal exception is the SPT-3G+BAO bound, which suggests that when large-scale CMB information from *Planck* is not included,³ the data struggle to break parameter degeneracies [55].

One may also add to CMB and BAO data another probe of the late background expansion in the form of measurements of the distance to uncalibrated type Ia supernovae (SNIa). However, this does not change much the constraining power on $N_{\rm eff}$, as shown for instance in Ref. [56]. Finally, one may also add information from large-scale structure (LSS), *i.e.*, on the growth rate and clustering amplitude of matter as a function of scale, although the DESI DR1 analysis [58] shows that LSS data are not very constraining for the $N_{\rm eff}$ parameter.

The situation is different with the inclusion of low-redshift measurements of H_0 with distance ladders (DLs) [59–61], reaching up to 5.7 σ tension with Planck in the Λ CDM framework. As explained in Section 26.2, the positive correlation between $N_{\rm eff}$ and h means that inclusion of the H_0 measurement would tend to push $N_{\rm eff}$ to higher values. However, the high values of $N_{\rm eff}$ needed to accommodate $H_0 \sim 73$ km/s/Mpc, as well as the sound horizon scale as seen in the CMB and BAO, are excluded by the measurement of the damping tail of the CMB temperature spectrum by Planck, ACT and/or SPT-3G.

Thus, the $N_{\rm eff}$ extension to the $\Lambda{\rm CDM}$ model does not reduce the tension significantly, and the combination of Planck and DL data does not return any meaningful constraint on $N_{\rm eff}$ in this context. It is currently unclear whether a resolution of the Hubble tension would require a departure from the $\Lambda{\rm CDM}$ (or $\Lambda{\rm CDM} + N_{\rm eff}$) model [11–13,62–66].

As long as DL data are not included, the error bars on $N_{\rm eff}$ degrade mildly when the data are analysed in the context of more extended cosmological scenarios. Adding only the total neutrino mass as an 8th free parameter has a negligible impact on the bounds [56]. The authors of Ref. [67] take a more extreme point of view and fit a 12-parameter model to Pl18[TT,TE,EE+lowE+lensing] data; they obtain $N_{\rm eff} = 2.95 \pm 0.24$ (68% CL), showing that it is very difficult with current cosmological data to accommodate shifts of more than 0.5 from the standard $N_{\rm eff}$ value, and to obtain good fits with, for instance, a fourth (sterile) thermalized neutrino. This is interesting, since the anomalies in some oscillation data could be interpreted as evidence for at least one sterile neutrino with a large mixing angle, which would need to be thermalised unless non-standard interactions come into play [5]. In other words, cosmology disfavours the explanation of the oscillations anomalies in terms of extra neutrinos if they are thermalized.

However, if a resolution to current tensions among cosmological data sets requires a departure from the Λ CDM model or its most simple extensions, the situation is more open. In the presence of new physical ingredients (such as non-standard interactions, exotic dark matter candidates, non-minimal dark energy properties, or modified gravity), it is in principle conceivable that $N_{\rm eff}$ reaches larger values. Still, within the w_0w_a CDM model (a dynamical dark energy extension to the Λ CDM model favored by some data set combinations, see Chap. 28 of this Review), the $N_{\rm eff}$ constraints do not change appreciably, as illustrated by the last bound quoted in Table 26.1.

26.3.2 Are they really neutrinos, as expected?

While a value of $N_{\rm eff}$ significantly different from zero (at more than 15σ) and consistent with the expected number 3.044 yields a powerful indirect confirmation of the $C\nu B$, departures from standard $N_{\rm eff}$ could be caused by any ingredient affecting the early-time expansion rate of the Universe. Extra relativistic particles (either decoupled, self-interacting, or interacting with a dark sector), a background of gravitational waves, an oscillating scalar field with quartic potential,

³The SPT-3G+DESI data set uses no information on CMB multipoles $\ell < 400$ but includes a prior on the optical depth to reionization inferred from low- ℓ Planck data [55].

departures from Einstein gravity, or large extra dimensions are some of the possibilities for such ingredients. In principle one could even assume that the $C\nu B$ never existed or has decayed (like in the "neutrinoless Universe" model of Ref. [68]), while another dark radiation component is responsible for $N_{\rm eff}$. At least, cosmological data allow to narrow the range of possible interpretations of $N_{\rm eff} \simeq 3$ to the presence of decoupled relativistic relics like standard neutrinos. Indeed, free-streaming particles leave specific signatures in the CMB and LSS spectra, because their density and pressure perturbations, bulk velocities, and anisotropic stress also source the metric perturbations. These signatures can be tested in several ways.

A first approach consists of introducing a self-interaction term in the neutrino equations [6,7]. Reference [8] finds that current CMB and BAO data are compatible with no self-interactions. The upper limit to the effective coupling constant G_{eff} for a Fermi-like four-fermions interaction at 95% confidence is $\log_{10}(G_{\text{eff}}\text{MeV}^2) < -1.47$ for Pl18+BAO [11]. Note, however, that neutrino self-interactions as strong as $\log_{10}(G_{\text{eff}}\text{MeV}^2) \simeq -1.4$ could reconcile CMB temperature and BAO data with the direct H_0 measurement of Ref. [69], but such interactions seem to be incompatible with BBN, laboratory constraints [10], and CMB polarization [9,11].

A second approach consists of introducing two phenomenological parameters, $c_{\rm eff}$ and $c_{\rm vis}$ (see e.g., Ref. [70–72]): $c_{\rm eff}^2$ generalizes the linear relation between isotropic pressure perturbations and density perturbations; and $c_{\rm vis}^2$ modifies the neutrino anisotropic stress equation. While relativistic free-streaming species have $(c_{\rm eff}^2, c_{\rm vis}^2) = (1/3, 1/3)$, a perfect relativistic fluid would have $(c_{\rm eff}^2, c_{\rm vis}^2) = (1/3, 0)$. Other values do not necessarily refer to a concrete model, but make it possible to interpolate between these limits. Planck data, alone or in combination with galaxy clustering, strongly suggests $(c_{\rm eff}^2, c_{\rm vis}^2) = (1/3, 1/3)$ [73–75].

Finally, Ref. [28] (Ref. [29]) shows that current data are precise enough to detect the "neutrino drag" effect mentioned in Sec. 26.2 through the measurement of the CMB peak (BAO) scale. These findings show that current cosmological data are able to detect not just the average density of some relativistic relics, but also their anisotropies.

26.3.3 Neutrino masses

Table 26.2: Summary of $\sum m_{\nu}$ constraints (95%CL).

| | Model | (eV) | Ref. |
|---|-------------------------------------|---------|------|
| CMB alone | | | |
| WMAP[T&E] | $\Lambda \text{CDM} + \sum m_{\nu}$ | < 1.3 | [76] |
| Pl18[T&E] | $\Lambda \text{CDM} + \sum m_{\nu}$ | < 0.26 | [53] |
| Pl18[T&E+lensing] | $\Lambda \text{CDM} + \sum m_{\nu}$ | < 0.24 | [53] |
| Pl18[T&E] + ACT[T&E] + SPT-3G[T&E, lensing] | $\Lambda \text{CDM} + \sum m_{\nu}$ | < 0.17 | [55] |
| $\overline{\mathrm{CMB} + \mathrm{BAO}}$ | | | |
| Pl18[T&E]+ACT[T&E,lensing]+DESI-DR2 | $\Lambda \text{CDM} + \sum m_{\nu}$ | < 0.077 | [77] |
| Pl18[T&E] + ACT[T&E] + SPT-3G[T&E, lensing] + DESI-DR2 | $\Lambda \text{CDM} + \sum m_{\nu}$ | < 0.048 | [55] |
| Pl18[T&E] + ACT[T&E, lensing] + DESI-DR2 | w_0w_a CDM+ $\sum m_{\nu}$ | < 0.186 | [77] |
| $\overline{\mathrm{CMB} + \mathrm{BAO} + \mathrm{LSS}}$ | | | |
| Pl18[T&E]+ACT[lensing]+DESI-DR1[BAO,FS] | $\Lambda \text{CDM} + \sum m_{\nu}$ | < 0.071 | [58] |
| $\underline{PR4[T\&E] + ACT[lensing] + DESI-DR1[BAO] + Lyman-\alpha}$ | $\Lambda \text{CDM} + \sum m_{\nu}$ | < 0.053 | [78] |

Table 26.2 shows a list of constraints on $\sum m_{\nu}$ obtained with several combinations of data sets. 'WMAP' denotes the Wilkinson Microwave Anisotropy Probe. The acronyms 'Pl18', 'ACT', 'SPT-3G', 'DESI-DR1' and 'DESI-DR2' have been described in the previous subsection. 'PR4' refers to

Planck Release 4 data analysed with the 'CamSpec' likelihood [79]. 'DESI-DR1[BAO-FS]' denotes the combined measurement of the BAO scale and full-shape matter power spectrum from DESI DR1 data [58], and 'Lyman-α' the one-dimensional flux power spectrum of eBOSS quasars analyzed with a new inference pipeline called 'Lyssa' in Ref. [78].

Given that most determinations of N_{eff} are compatible with the standard prediction, $N_{\text{eff}} = 3.044$, it is reasonable to adopt this value as a theoretical prior and to investigate neutrino mass constraints in the context of a minimal 7-parameter model, $\Lambda \text{CDM} + \sum m_{\nu}$.

Firstly, an extremely robust bound comes from WMAP data (or Planck data limited to large angular scales), which constrain neutrino masses mainly through the non-detection of the very specific neutrino-induced early ISW effect mentioned in Sec. 26.2.3, and set $\sum m_{\nu} < 1.3 \,\mathrm{eV}$ (95%CL) [76]. Assuming a minimal 7-parameter model, the next most conservative constraint arises from Planck 2018 temperature and polarization data alone: $\sum m_{\nu} < 0.26 \,\mathrm{eV}$ (95%CL) [53]. Among the four effects of neutrino masses on the CMB spectra described before, Planck (and post-Planck) bounds are dominated by the first and the third effects (modified late background evolution, and distortions of the temperature and polarization spectra through weak lensing) – as discussed, e.g., in Refs. [32, 80, 81]. It is worth noticing that the actual *Planck* bound depends on the version of the *Planck* data release and likelihood that one adopts (see, e.g., Ref. [81]). As a matter of fact, different versions suggest a slightly different amplitude for the distortions induced in the high- ℓ temperature spectrum by weak lensing. However, all versions of *Planck* and of other CMB high- ℓ likelihoods agree on the fact that there is a high level of such distortions. These are compatible with a large amplitude of the matter power spectrum and a negligible impact of neutrino free-streaming. This feature tightens any neutrino mass bound based on high-\ell temperature data. Complementing Planck data with recent measurements of high-ℓ temperature and polarization from ACT and SPT-3G further tightens the bounds. On the other hand, adding independent information on the CMB lensing potential inferred from CMB lensing extraction has a moderate impact. The CMB-only bound from combined Planck 2018, ACT, and SPT-3G data (including CMB lensing) is as strong as $\sum m_{\nu} < 0.17 \text{ eV } (95\%\text{CL})$ [55].

Adding measurements of the BAO scale is crucial, since the comparison between the angular diameter distance $d_{\rm A}(z)$ to small and large redshifts makes it possible to break parameter degeneracies, for instance between $\sum m_{\nu}$ and H_0 . However, neutrino mass bounds from BAOs are very model dependent, since the impact of massive neutrinos on the angular distance is not specific and could be confused, for instance, with dynamical dark energy. The combination of *Planck* and ACT with BAO measurements from DESI DR2 provides a strong bound, $\sum m_{\nu} < 0.077 \text{ eV } (95\%\text{CL})$ [77]. In this case, Planck high- ℓ data are no longer playing a crucial role: one gets essentially the same result when keeping only the low- ℓ polarization information from Planck [77]. The bound narrows down to $\sum m_{\nu} < 0.048 \text{ eV } (95\%\text{CL})$ when also adding recent SPT-3G data [55], which may appear like a tension with the minimal value of the summed mass allowed by oscillation experiments (when assuming Λ CDM).⁴ The reason is that current CMB temperature and BAO data are better fit by models with slightly more CMB lensing and a slightly different expansion rate than in the Λ CDM model with massless neutrinos. Increasing the neutrino mass tends to worsen the fit to both data sets. Recently, some authors (see, e.g., [80]) discussed models with an unphysical "negative neutrino mass". This should be interpreted as follows: if the current trends in the data get confirmed, and the minimal Λ CDM model needs to be extended with a new ingredient, this ingredient should have an effect on CMB lensing and on the expansion rate opposite to that of neutrino masses. Dynamical dark energy is an example of such extension. The model dependence of the CMB+BAO mass bounds becomes clear when considering for instance that, in the $w_0 w_a \text{CDM}$ model, the combined *Planck*, ACT, SPT-3G, and DESI-DR2 bound relaxes to $\sum m_{\nu} < 0.186$ eV (95%CL) [77].

⁴All the bounds reported here are obtained under the agnostic prior $\sum m_{\nu} > 0$.

In addition to CMB+BAO data, one could add further information on the late background expansion from uncalibrated SNIa luminosity. Here, we refrain from quoting such bounds due to the moderate tension between current CMB, BAO, and SNIa data in the minimal 7-parameter model [58]. Similarly, because the parameter correlation between $\sum m_{\nu}$ and H_0 is negative, the inclusion of DL data would tend to provide stronger bounds on neutrino masses. However, like for N_{eff} , such bounds would not be meaningful, since they would arise from a combination of discrepant data sets.

To mitigate the model dependence of CMB+BAO bounds, it would in principle be crucial to include LSS data sets, directly sensitive to the small-scale suppression of the matter power spectrum due to neutrino free-streaming. Current mass bounds are still dominated by information on the expansion history and CMB lensing, but LSS data are increasingly constraining. Adding the full-shape information on the matter power spectrum measured by DESI-DR1 shrinks the Planck+ACT+BAO 95%CL bound from 0.082 eV to 0.071 eV [58]. Combining the same CMB+BAO data set with eBOSS Lyman- α data brings the bound down to 0.053 eV [78]. However, these bounds relax considerably when BAO information is omitted, and are thus still very model dependent. Finally, one may add information on the amplitude of the matter power spectrum coming from weak lensing surveys. The most recent measurements from DES [82] or KiDS [83] are in good agreement with the massless Λ CDM model inferred from CMB data, and as such, do not have a strong impact on neutrino mass bounds compared to CMB+BAO.

One should stress again that if the explanation of DL measurements (or of recent BAO and SNIa data) requires a cosmological scenario with new – and yet unknown – physical ingredients, the current neutrino mass bounds may in principle be shifted or relaxed. We have quoted a few weaker bounds assuming a particular parameterization of dynamical dark energy. However, in the absence of working scenarios that convincingly explain the Hubble tension without raising other tensions, we do not at the moment have any framework for quoting alternative mass bounds compatible with all current data sets.

26.4 Future prospects and outlook

The cosmic neutrino background has been detected indirectly at very high statistical significance. Direct detection experiments are now being planned, e.g., at the Princeton Tritium Observatory for Light, Early Universe, Massive-neutrino Yield (PTOLEMY) [84]. The detection prospects crucially depend on the exact value of neutrino masses and on the enhancement of their density at the location of the Earth through gravitational clustering in the Milky Way and its sub-halos – an effect, however, that is expected to be small [85–88].

Over the past few years the upper limit on the sum of neutrino masses has become increasingly stringent, first indicating that the mass ordering is hierarchical, then putting the inverted hierarchy under pressure, and now even possibly starting to question the normal hierarchy. However, these bounds rely on the Λ CDM model, and thus, on the assumption that a resolution of the Hubble tension with DL measurements (or of a possible tension on the late expansion history with BAO and SNIa measurements) does not affect the modeling and interpretation of the data sets adopted here. If this is not the case, a shift of paradigm might be required, potentially leading to weaker neutrino density and mass bounds.

Neutrino mass and number of species bounds are expected to keep improving significantly over the next years, thanks to new LSS experiments like Euclid [89], Roman [90], SPHEREx [91] and SKA [92], in combinations with new CMB experiments like Simons Observatory [93] or LiteBird [94]. If the Λ CDM model is confirmed, and if neutrinos have standard properties, the total neutrino mass should be detected at the level of at least 3–4 σ even at the minimum level allowed by oscillations. This is the conclusion reached by several independent studies, using different data set combinations

(see e.g., [43,95–100]). One should note that at the minimum level allowed by oscillations $\sum m_{\nu} \simeq 0.06 \,\text{eV}$, neutrinos constitute about 0.5% of the Universe matter density, and their effects on the matter power spectrum are only at the 5% level, implying that exquisite control of systematic errors will be crucial to achieve the required accuracy. At this level, the information coming from the power spectrum shape will be more powerful than that coming from geometrical measurements (e.g., BAO). But exploiting the shape information, especially on small, mildly non-linear or non-linear scales, requires improved understanding of the non-linear regime, and of galaxy bias for galaxy surveys. The fact that different surveys, different probes, and different data set combinations have enough statistical power to reach this level, offers a much needed redundancy and the possibility to perform consistency checks, which in turns helps immensely with the control of systematic errors and in making the measurement robust. Using the entire Universe as a particle detector, the ongoing and future observational efforts hold the exciting prospect of providing a measurement of the sum of neutrino masses and possibly an indication of their mass hierarchy.

References

- [1] A. D. Dolgov, Phys. Rept. **370**, 333 (2002), [hep-ph/0202122].
- [2] J. Lesgourgues and S. Pastor, Phys. Rept. **429**, 307 (2006), [arXiv:astro-ph/0603494].
- [3] S. Hannestad, Prog. Part. Nucl. Phys. 65, 185 (2010), [arXiv:1007.0658].
- [4] J. Lesgourgues et al., Neutrino Cosmology, Cambridge University Press (2013), ISBN 978-1-108-70501-1, 978-1-139-60341-6.
- [5] M. Archidiacono et al., JCAP **1608**, 08, 067 (2016), [arXiv:1606.07673].
- [6] L. Lancaster et al., JCAP 1707, 07, 033 (2017), [arXiv:1704.06657].
- [7] I. M. Oldengott et al., JCAP 1711, 11, 027 (2017), [arXiv:1706.02123].
- [8] M. Park et al., Phys. Rev. D 100, 6, 063524 (2019), [arXiv:1904.02625].
- [9] C. D. Kreisch, F.-Y. Cyr-Racine and O. Doré, Phys. Rev. D 101, 12, 123505 (2020), [arXiv:1902.00534].
- [10] N. Blinov et al., Phys. Rev. Lett. 123, 19, 191102 (2019), [arXiv:1905.02727].
- [11] N. Schöneberg et al., Phys. Rept. **984**, 1 (2022), [arXiv:2107.10291].
- [12] A. R. Khalife et al., JCAP **04**, 059 (2024), [arXiv:2312.09814].
- [13] E. Di Valentino *et al.* (CosmoVerse Network), Phys. Dark Univ. **49**, 101965 (2025), [arXiv:2504.01669].
- [14] J. Birrell, C.-T. Yang and J. Rafelski, Nucl. Phys. **B890**, 481 (2014), [arXiv:1406.1759].
- [15] G. Mangano et al., Nucl. Phys. **B729**, 221 (2005), [hep-ph/0506164].
- [16] E. Grohs et al., Phys. Rev. **D93**, 8, 083522 (2016), [arXiv:1512.02205].
- [17] P. F. de Salas and S. Pastor, JCAP **1607**, 07, 051 (2016), [arXiv:1606.06986].
- [18] J. Froustey, C. Pitrou and M. C. Volpe, JCAP 12, 015 (2020), [arXiv:2008.01074].
- [19] J. J. Bennett et al., JCAP **04**, 073 (2021), [arXiv:2012.02726].
- [20] M. Cielo et al., Phys. Rev. D 108, 12, L121301 (2023), [arXiv:2306.05460].
- [21] K. Akita and M. Yamaguchi, JCAP 08, 012 (2020), [arXiv:2005.07047].
- [22] T. Binder et al. (2024), [arXiv:2411.14091].
- [23] J. Froustey, The Universe at the MeV era: neutrino evolution and cosmological observables, Ph.D. thesis, Institut d'Astrophysique de Paris, France, Paris, Inst. Astrophys. (2022), [arXiv:2209.06672].

- [24] S. Bashinsky and U. Seljak, Phys. Rev. **D69**, 083002 (2004), [arXiv:astro-ph/0310198].
- [25] Z. Hou et al., Phys. Rev. **D87**, 083008 (2013), [arXiv:1104.2333].
- [26] J. Lesgourgues et al., Neutrino cosmology (Cambridge University Press, 2013).
- [27] M. M. Saravanan et al., JCAP 08, 040 (2025), [arXiv:2503.04671].
- [28] B. Follin et al., Phys. Rev. Lett. 115, 9, 091301 (2015), [arXiv:1503.07863].
- [29] D. Baumann et al., Nature Phys. 15, 465 (2019), [arXiv:1803.10741].
- [30] A. Lewis and A. Challinor, Phys. Rept. 429, 1 (2006), [arXiv:astro-ph/0601594].
- [31] Z. Hou et al., Astrophys. J. **782**, 74 (2014), [arXiv:1212.6267].
- [32] M. Loverde and Z. J. Weiner, JCAP **12**, 048 (2024), [arXiv:2410.00090].
- [33] J. Lesgourgues and S. Pastor, Adv. High Energy Phys. **2012**, 608515 (2012), [arXiv:1212.6154].
- [34] J. R. Bond, G. Efstathiou and J. Silk, Phys. Rev. Lett. 45, 1980 (1980), [,61(1980)].
- [35] W. Hu, D. J. Eisenstein and M. Tegmark, Phys. Rev. Lett. 80, 5255 (1998), [arXiv:astro-ph/9712057].
- [36] S. Bird, M. Viel and M. G. Haehnelt, Mon. Not. Roy. Astron. Soc. 420, 2551 (2012), [arXiv:1109.4416].
- [37] C. Wagner, L. Verde and R. Jimenez, Astrophys. J. 752, L31 (2012), [arXiv:1203.5342].
- [38] C. J. Todero Peixoto, V. de Souza and P. L. Biermann, JCAP **1507**, 07, 042 (2015), [arXiv:1502.00305].
- [39] J. Brandbyge and S. Hannestad, JCAP 1710, 10, 015 (2017), [arXiv:1706.00025].
- [40] J. Adamek, R. Durrer and M. Kunz, JCAP 1711, 11, 004 (2017), [arXiv:1707.06938].
- [41] M. Archidiacono et al., JCAP 1702, 02, 052 (2017), [arXiv:1610.09852].
- [42] A. Liu et al., Phys. Rev. **D93**, 4, 043013 (2016), [arXiv:1509.08463].
- [43] R. Allison et al., Phys. Rev. **D92**, 12, 123535 (2015), [arXiv:1509.07471].
- [44] J. Lesgourgues, S. Pastor and L. Perotto, Phys. Rev. **D70**, 045016 (2004), [hep-ph/0403296].
- [45] A. Slosar, Phys. Rev. **D73**, 123501 (2006), [arXiv:astro-ph/0602133].
- [46] R. Jimenez et al., JCAP **1005**, 035 (2010), [arXiv:1003.5918].
- [47] R. Jimenez, C. P. Garay and L. Verde, Phys. Dark Univ. 15, 31 (2017), [arXiv:1602.08430].
- [48] A. F. Heavens and E. Sellentin, JCAP **04**, 047 (2018), [arXiv:1802.09450].
- [49] M. Archidiacono, S. Hannestad and J. Lesgourgues, JCAP 09, 021 (2020), [arXiv:2003.03354].
- [50] F. Capozzi et al., Phys. Rev. D 104, 8, 083031 (2021), [arXiv:2107.00532].
- [51] R. Jimenez et al., JCAP **09**, 006 (2022), [arXiv:2203.14247].
- [52] S. Gariazzo, O. Mena and T. Schwetz, Phys. Dark Univ. **40**, 101226 (2023), [arXiv:2302.14159].
- [53] N. Aghanim et al. (Planck), Astron. Astrophys. 641, A6 (2020), [Erratum: Astron. Astrophys. 652, C4 (2021)], [arXiv:1807.06209].
- [54] E. Calabrese et al. (ACT) (2025), [arXiv:2503.14454].
- [55] E. Camphuis et al. (SPT-3G) (2025), [arXiv:2506.20707].
- [56] W. Elbers et al. (DESI) (2025), [arXiv:2503.14744].
- [57] M. Abdul Karim et al. (DESI) (2025), [arXiv:2503.14738].

- [58] A. G. Adame et al. (DESI), JCAP 07, 028 (2025), [arXiv:2411.12022].
- [59] A. G. Riess et al., Astrophys. J. Lett. 934, 1, L7 (2022), [arXiv:2112.04510].
- [60] Y. S. Murakami et al., JCAP 11, 046 (2023), [arXiv:2306.00070].
- [61] W. L. Freedman et al., Astrophys. J. 985, 2, 203 (2025), [arXiv:2408.06153].
- [62] J. L. Bernal, L. Verde and A. G. Riess, JCAP 1610, 10, 019 (2016), [arXiv:1607.05617].
- [63] L. Verde, T. Treu and A. G. Riess, Nature Astron. 3, 891 (2019), [arXiv:1907.10625].
- [64] J. L. Bernal et al., Phys. Rev. D 103, 10, 103533 (2021), [arXiv:2102.05066].
- [65] E. Di Valentino et al., Class. Quant. Grav. 38, 15, 153001 (2021), [arXiv:2103.01183].
- [66] E. Abdalla et al., JHEAp **34**, 49 (2022), [arXiv:2203.06142].
- [67] E. Di Valentino, A. Melchiorri and J. Silk, JCAP **01**, 013 (2020), [arXiv:1908.01391].
- [68] J. F. Beacom, N. F. Bell and S. Dodelson, Phys. Rev. Lett. 93, 121302 (2004), [arXiv:astro-ph/0404585].
- [69] A. G. Riess et al., Astrophys. J. Lett. 908, 1, L6 (2021), [arXiv:2012.08534].
- [70] W. Hu, Astrophys. J. **506**, 485 (1998), [arXiv:astro-ph/9801234].
- [71] W. Hu et al., Phys. Rev. D59, 023512 (1999), [arXiv:astro-ph/9806362].
- [72] M. Gerbino, E. Di Valentino and N. Said, Phys. Rev. **D88**, 6, 063538 (2013), [arXiv:1304.7400].
- [73] B. Audren et al., JCAP **1503**, 036 (2015), [arXiv:1412.5948].
- [74] P. A. R. Ade et al. (Planck), Astron. Astrophys. **594**, A13 (2016), [arXiv:1502.01589].
- [75] S. Kumar, R. C. Nunes and P. Yadav, JCAP **09**, 060 (2022), [arXiv:2205.04292].
- [76] G. Hinshaw et al. (WMAP), Astrophys. J. Suppl. 208, 19 (2013), [arXiv:1212.5226].
- [77] C. Garcia-Quintero et al. (DESI) (2025), [arXiv:2504.18464].
- [78] D. Chebat et al. (2025), [arXiv:2507.12401].
- [79] E. Rosenberg, S. Gratton and G. Efstathiou, Mon. Not. Roy. Astron. Soc. 517, 3, 4620 (2022), [arXiv:2205.10869].
- [80] W. Elbers et al., Phys. Rev. D 111, 6, 063534 (2025), [arXiv:2407.10965].
- [81] D. Naredo-Tuero et al., Phys. Rev. D 110, 12, 123537 (2024), [arXiv:2407.13831].
- [82] T. M. C. Abbott et al. (DES), Phys. Rev. D 105, 2, 023520 (2022), [arXiv:2105.13549].
- [83] A. H. Wright et al. (2025), [arXiv:2503.19441].
- [84] S. Betts et al., in "Proceedings, 2013 Community Summer Study on the Future of U.S. Particle Physics: Snowmass on the Mississippi (CSS2013): Minneapolis, MN, USA, July 29-August 6, 2013," (2013), [arXiv:1307.4738], URL http://www.slac.stanford.edu/econf/C1307292/ docs/submittedArxivFiles/1307.4738.pdf.
- [85] A. Ringwald and Y. Y. Y. Wong, JCAP **0412**, 005 (2004), [hep-ph/0408241].
- [86] F. Villaescusa-Navarro et al., JCAP 1303, 019 (2013), [arXiv:1212.4855].
- [87] P. F. de Salas et al., JCAP **1709**, 09, 034 (2017), [arXiv:1706.09850].
- [88] M. Bauer and J. D. Shergold, JCAP **01**, 003 (2023), [arXiv:2207.12413].
- [89] R. Laureijs et al. (EUCLID) (2011), [arXiv:1110.3193].
- [90] Paul A. Abell *et al.*, LSST Science and LSST Project Collaborations, http://lss.fnal.gov/archive/test-tm/2000/fermilab-tm -2495-a.pdf (2009) arXiv:0912.0201.

- [91] J. Bock and SPHEREx Science Team, in "American Astronomical Society Meeting Abstracts #231," volume 231 of American Astronomical Society Meeting Abstracts, 354.21 (2018).
- [92] http://www.skatelescope.org.
- [93] P. Ade et al. (Simons Observatory), JCAP **02**, 056 (2019), [arXiv:1808.07445].
- [94] M. Hazumi et al., J. Low Temp. Phys. **194**, 5-6, 443 (2019).
- [95] C. Carbone et al., JCAP **1103**, 030 (2011), [arXiv:1012.2868].
- [96] J. Hamann, S. Hannestad and Y. Y. Y. Wong, JCAP **1211**, 052 (2012), [arXiv:1209.1043].
- [97] B. Audren et al., JCAP 1301, 026 (2013), [arXiv:1210.2194].
- [98] R. Pearson and O. Zahn, Phys. Rev. **D89**, 4, 043516 (2014), [arXiv:1311.0905].
- [99] F. Villaescusa-Navarro, P. Bull and M. Viel, Astrophys. J. **814**, 2, 146 (2015), [arXiv:1507.05102].
- [100] T. Brinckmann et al., JCAP 1901, 059 (2019), [arXiv:1808.05955].